CFD Modelling of Wind Farms in Flat and Complex Terrain

J. M. Prospathopoulos[1] jprosp@cres.gr
E. S. Politis[1] vpolitis@cres.gr
P. K. Chaviaropoulos[1] tchaviar@cres.gr
K. G. Rados[2] kgrados@teikoz.gr
J. G. Schepers[3] schepers@ecn.nl
D. Cabezon[4] dcabezon@cener.com
K. S. Hansen[5] ksh@mek.dtu.dk
R. J. Barthelmie[6] rbarthel@indiana.edu

[1]: Centre of Renewable Energy Sources
[2]: School of Mechanical Engineering, National Technical University of Athens
[3]: Energy research Centre of the Netherlands
[4]: National Renewable Energy Centre of Spain
[5]: Department of Mechanical Engineering, Technical University of Denmark
[6]: Atmospheric Science and Sustainability, Department of Geography, Indiana University

Abstract:

Modelling of entire wind farms in flat and complex terrain using a full 3D Navier–Stokes solver for incompressible flow is presented in this paper. Numerical integration of the governing equations is performed using an implicit pressure correction scheme, where the wind turbines (W/Ts) are modelled as momentum absorbers through their thrust coefficient. The *k–ω* turbulence model, suitably modified for atmospheric flows, is employed for closure. A correction is introduced to account for the underestimation of the near wake deficit, in which the turbulence time scale is bounded using a general "realizability" constraint for the fluctuating velocities. The second modelling issue that is discussed in this paper is related to the determination of the reference wind speed for the thrust calculation of the machines. Dealing with large wind farms and wind farms in complex terrain, determining the reference wind speed is not obvious when a W/T operates in the wake of another WT and/or in complex terrain. Two alternatives are compared: using the wind speed value at hub height one diameter upstream of the W/T and adopting an induction factor-based concept to overcome the utilization of a wind speed at a certain distance upwind of the rotor. Application is made in two wind farms, a five-machine one located in flat terrain and a 43-machine one located in complex terrain.

Keywords: Wind farm CFD modelling, wind turbine wakes, induction factor, *k–ω* turbulence model, Durbin's correction.

1 Introduction

Wind energy community has an increasing interest in wake modelling for two main reasons. Obviously, accurately quantifying power losses due to wind turbine wakes is an important part of the overall wind farm economics. In parallel, the need for maximizing the deployment of wind energy leads to installing machines at the closest possible distances, increasing thus the interaction phenomena and affecting the performance of the downstream turbines by reducing their power output and increasing the fluctuating loads.

During the last 25 years researchers have been developing models for the simulation of wind turbine wakes. At a first stage, many simple kinematic models appeared in the literature [1], [2], which were based on Gaussian-type velocity deficit profiles stemming from experimental and theoretical works [3]. A step further was the numerical calculation of the flow field using two-dimensional or axisymmetric models, which better represent the physical mechanisms that govern the wake development. In this context, methodologies varied from the boundary layer [4] and the parabolic approximation [5] of the linearized momentum equations to the solution of the axisymmetric Navier–Stokes equations. A common difficulty in all these models was the initialization of the velocity deficit profile. For example, the axisymmetric Navier–Stokes solver of Garrad Hassan & Partners Ltd. [6], with an eddy-viscosity closure, was initiated at a distance of two diameters behind the rotor using an empirical wake profile. Some hybrid methodologies were also developed

suggesting a solution to the problem of the velocity profile initialization. Voutsinas et al. [7] applied a vortex-particle method in the rotor region to model the initial wake development. The near-wake region was simulated with a field model whilst self-similar expressions were applied in the far-wake region.

During the last decade, the rapid development of the computer technology has allowed the use of more advanced CFD methodologies, such as the solution of the full 3D Navier–Stokes equations combined with the actuator disk [8] or the actuator line [9] techniques for the simulation of a W/T rotor. An obvious merit of the inherent modelling of the W/T rotor disk is that it allows the prediction of the flow in the wake without using any initial velocity deficit profile.

The aforementioned methodologies have constituted the basis for the development of several wind farm models. An assessment of wind farm models, from the simplest to the most advanced ones, has been carried out in the context of the EC-funded UpWind project using experimental data from the Danish offshore wind farm Horns Rev [10]. The degree of complexity of the reviewed models starts from the well known and straightforward WAsP model [11], increases to the moderately complex Ainsle-based WindFarmer [12], to the more complex WAKEFARM [13], that is based on the parabolized Navier–Stokes equations, and finally reaches the advanced Fluent and 3D–NS [14] models, which solve the complete 3D Navier–Stokes equations. Predictions were compared with measurements for the wind direction of 270^o at various sector widths in the range of $\pm 1^o$ to $\pm 15^o$. Despite the fact that a thorough assessment turned out to be extremely difficult due to the large uncertainties of the measurement data due to the atmospheric conditions, the preliminary results showed that the CFD models over-predicted wake losses in the narrow sectors, while the simpler wind farm models tended to under-predict wake losses unless their coefficients were calibrated to match the observations.

The present paper deals with the wind farm modelling through full 3D Navier–Stokes solvers. Such a solver, incorporating the *k–ω* turbulence model, suitably modified for atmospheric flows, is applied to the simulation of two wind farms, one in flat and the one complex terrain. The WTs are modelled as momentum sinks through their thrust coefficient. The aim of the work is to contribute to the wake modelling through CFD solvers by investigating two basic modelling issues. The first issue is related to the underestimation of the near wake deficit appearing in the simulations when compared to the measurements. In this context, a turbulence correction is applied using a general "realizability" constraint for the fluctuating velocities. The second issue is the derivation of the reference wind speed for the calculation of the thrust of the W/Ts. In this context, an induction factor-based concept is applied, which has the advantage of not using the wind speed at a specific distance upwind of a modelled rotor. Results by this approach are compared with results using the wind speed value at hub height one diameter upstream of the W/T as a reference wind speed, which is the obvious choice for single wake simulations in flat terrain.

2 The numerical model

CRES–flowNS [15] is a 3D Navier–Stokes solver using the *k-ω* turbulence model. The momentum equations are numerically integrated introducing a matrix-free pressure correction algorithm which maintains the compatibility of the velocity and pressure field corrections. Discretization is performed with a finite volume technique using a body-fitted coordinate transformation on a curvilinear mesh. Convection terns are handled by a second order upwind scheme bounded through a limiter, whereas centred second order schemes are employed for the diffusion terms. Velocity-pressure decoupling is prevented by a linear fourth order dissipation term added into the continuity equation.

The *k-ω* turbulence model is suitably modified for neutral atmospheric conditions [16]:

$$\alpha = 0.3706, \quad \beta = 0.0275, \quad \beta_* = 0.033, \quad \sigma = 0.5, \quad \sigma_* = 0.5 \tag{1}$$

For stable atmospheric conditions, a production term is added to the *k* equation to account for the buoyancy effect [12]:

$$G = -\mu_t \left(\frac{\partial U}{\partial z} \right)^2 \cdot \frac{Ri}{f_m}, \tag{2}$$

where the Richardson number, *Ri*, is estimated as [17]:

$$Ri = \zeta \frac{0.74 + 4.7\zeta}{(1 + 4.7\zeta)^2} \tag{3}$$

and $f_m = 1 + 5\zeta$, with $\zeta = z / L$. The Monin-Obukhov length, *L*, characterizes the stability.

The inflow wind speed profile follows the logarithmic law of a fully developed boundary layer:

$$U_x = \frac{u_*}{K}\left[ln\left(z / z_0\right) + c\left(z\right)\right] \quad (4)$$

with $c(z) = 0$ and $c(z) = 5z / L$ for neutral and stable conditions, respectively. In Eq. (4) u_* stands for the friction velocity, *K* is the von-Karman constant and z_0 is the roughness length. The inflow profiles of *k* and *ω* are given by the relationships [18]:

$$k = \frac{u_*^2}{\sqrt{\beta_*}} \cdot \left(\frac{f_\omega}{f_m}\right)^{0.5} \quad (5)$$

and

$$\omega = \frac{u}{\sqrt{\beta_*} \cdot K \cdot z}\left(f_\omega \cdot f_m\right)^{0.5} \quad (6)$$

For neutral conditions, $f_m = f_\omega = 1$, whilst for stable conditions, $f_m = 1 + 5\zeta$ and $f_\omega = 1 + 4\zeta$.

The rotor disk of one W/T is discretized by a number of control volumes. Each control volume acts as a momentum sink through the actuator force calculated using the following relationship:

$$F = 0.5\rho\, U_{ref}^2\, C_T\, \Delta S \quad (7)$$

where *ρ* stands for the air density, U_{ref} is the reference wind speed for the thrust coefficient calculation, C_T is the thrust coefficient and ΔS is the surface area of the control volume. Stemming from the definition of the thrust coefficient, the common practice is to use as reference the wind speed value one diameter upwind of the rotor, either the value at hub height or the average over the rotor disk area. However, when a W/T is located in the wake of another W/T and/or the terrain is complex, this approach is doubtful, so an alternative one is discussed in Section 3.2.

3 Modelling issues

3.1 Near wake deficit correction

A significant underestimation of the near wake deficit has been reported in W/T simulations, especially in neutral atmospheric conditions [19]. This is attributed to the existence of a non-equilibrium region close to the turbine, where there is an enhancement of the turbulence dissipation rate. Several modelling remedies have been proposed to account for the physical mechanism delaying the wake flow recovery [20]. Their main deficiency is their dependence upon constants that need calibration using experimental data.

In the present work, a correction already used in stagnation point aerodynamic flows is adopted. It was suggested by Durbin [21] who noticed that two-equation turbulence models predict an anomalously large growth of turbulent kinetic energy in stagnation point flows, because of the erroneous normal stress difference produced by the eddy-viscosity formula. To ameliorate this anomaly, he set the so-called "realizability" constraint $2k \geq \overline{u^2} \geq 0$, where *u* can be any component of the fluctuating velocity. By applying this constraint on the eddy-viscosity formula written in the principal axes of the strain tensor, the following bound for the turbulent time scale is obtained:

$$T = min\left(\frac{1}{\omega}, \frac{2}{3}\sqrt{\frac{3}{8S^2}}\right), \quad (8)$$

where $S^2 = S_{ij} \cdot S_{ji}$ and S_{ij} is the strain tensor given by the relationship:

$$S_{ij} = \frac{1}{2}\left(\frac{\partial U_i}{\partial x_j} + \frac{\partial U_j}{\partial x_i}\right) \quad (9)$$

In Eq. (9) x_i are the Cartesian coordinates and U_i the velocity components. Eq. (8) can be used to substitute the turbulent time scale in the calculation of the turbulent viscosity and the *ω* transport equation. Owing to its generality, this constraint can be applied to any flow simulation, even in atmospheric flows and it can account even for steep topographies. It also features the advantage of not including any parameter that needs tuning. It should be noted though that the usual assumption in CFD wake modelling that the rotor is just acting as a momentum sink without any further influence on the Reynolds stress tensor is not affected by the present correction.

3.2 Thrust calculation

In order to estimate the actuator force in Eq. (7), the reference wind speed, U_{ref}, that corresponds to the thrust coefficient C_T must be defined. The common procedure is to use the wind speed value at one diameter upstream of the rotor disk. Then U_{ref} can be taken equal to the calculated wind speed value at the hub height or to the average value of the wind speed over the disk area. Considering that the trust coefficient of a wind turbine is

defined in single machine operation in flat terrain under uniform inflow conditions, this approximation can be considered as valid only in cases that the flow field upstream of the W/T is not affected by terrain and/or by the wakes of upstream or neighbouring W/Ts. So, in cases of complex terrain or multi-wake interactions, the derivation of the reference wind speed is not obvious.

In the present work, an alternative approach is tested, that is based on the induction factor concept. The induction factor of the actuator disk is defined as:

$$a = \frac{U_{ref} - U_{disk}}{U_{ref}} \Rightarrow U_{ref} = \frac{U_{disk}}{1-a} \qquad (10)$$

where U_{ref} is the, unknown, W/T reference wind speed and U_{disk} is the wind speed value at the hub height or the average wind speed over the rotor plane. Following the blade element momentum theory, the W/T thrust coefficient can be expressed as a function of the induction factor [22]:

$$C_T = \begin{cases} 4a(1-a), & a < 0.4 \\ 0.89 - \dfrac{0.20 - (a - 0.143)^2}{0.643}, & a \geq 0.4 \end{cases} \qquad (11)$$

The Eqs. (10) and (11), along with the thrust coefficient curve $C_T=C_T(U_{ref})$, can be solved iteratively to provide the value U_{ref}. This method has the advantage that the estimation of U_{ref} is not linked with a certain distance upstream of the W/T. However, it bears potential and uniform flow approximations due to the use of the induction factor relationships.

4 Application to wind farms

4.1 Wind farm in flat terrain

Application of the method is made on the ECN test farm [23] where 5 W/Ts, denoted as t5, t6, t7, t8 and t9 (with the respective power productions denoted as P5, P6, P7, P8 and P9) are positioned in a row. The diameter (D) and the hub height of the W/Ts are 80 m, while the distance between two successive W/Ts is 3.8 D. Calculations are performed for stable conditions and a range of wind directions from -30° to +30°, where 0° refer to the direction of the W/Ts' row.

The dimensions of the computational domain are extended sufficiently off the rotor planes so that the flow is not restricted by the computational boundaries, where Neumann conditions are imposed. For each wind direction, the coordinate system is selected so that its origin coincides with the position of the first W/T and the x- axis is aligned with the wind direction. The grid spacing is kept uniform, close to 0.05 D, between the W/Ts, and increases downstream of the last W/T, following a geometrical progression, until the maximum dimension of the domain is reached. Two-dimensional layouts of the generated mesh for the 0° and 30° wind direction cases are shown in Figure 1 and Figure 2, respectively.

In the vertical direction, the first three grid-surfaces are positioned close to the ground at heights of 0.01, 0.03 and 0.05 D, respectively. An equidistant fine mesh is constructed over the rotor disk areas. The grid density in these areas is chosen after checking the dependency of the predictions on the number of grid points for the 0° wind direction. Three different meshes have been used in that respect, with 15, 21 and 30 grid points across the rotor diameter. The difference in the power predictions between the two finer meshes is of the order of 1%, indicating that a number of 21 grid points across the rotor diameter is sufficient.

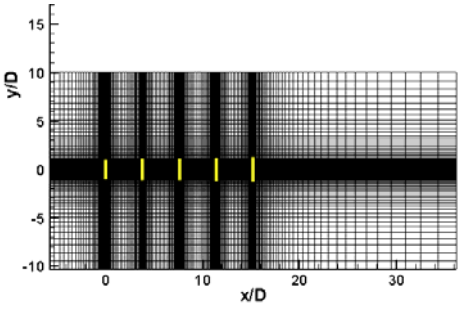

Figure 1: Two-dimensional layout of the generated grid for the simulation of the ECN test farm for 0° wind direction.

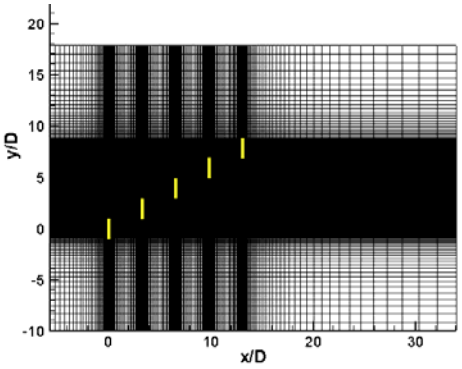

Figure 2: Two-dimensional layout of the generated grid for the simulation of the ECN test farm for 30° wind direction.

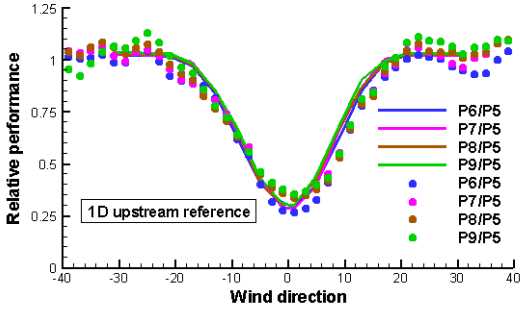

Figure 3: Relative power performances for the ECN test farm (U=6–8m/s). The reference wind speed is defined one diameter upstream of the rotor. Lines correspond to predictions, symbols to measurements.

The relative power performances for all W/Ts are plotted in Figure 3, as predicted when using as reference for the thrust calculation the average wind speed value at the rotor plane one diameter upstream of the rotor. Since this is the baseline simulation, the Durbins' correction is not included in the turbulence model. A reasonable quantitative agreement between predictions and measurements is observed. However, the under-performance of the second W/T, which is apparent in the measurements, is not reflected in the numerical predictions. The main deficiency of these predictions lies in the fact no over-prediction of the power of the WT's appears, as expected from reported single wake simulations [19].

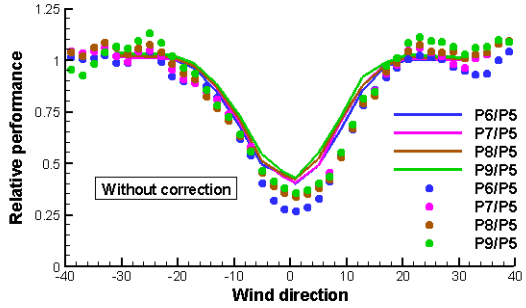

Figure 4: Relative power performances for the ECN test farm. The reference velocity is defined using the induction factor concept. Lines correspond to predictions, symbols to measurements.

The relative power predictions are also plotted in Figure 4, but in this simulation the induction factor method has been used for the estimation of the reference wind speed. Again, the Durbin's correction is not included in the turbulence model. Although that, with respect to the results shown in Figure 3, the agreement with the measurements is lower,

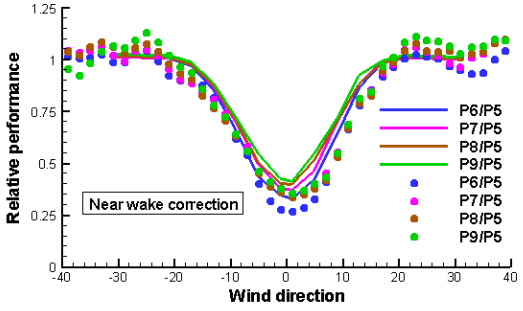

Figure 5: Relative power performances for the ECN test farm. The reference wind speed is defined using the induction factor concept. Correction of the turbulence model is applied.

the over-estimation of the power is in accordance to the predictions in single wake computations with two-equation turbulence models.

Finally, in the relative power performances for all W/Ts that are shown in Figure 5, the Durbin's correction has been included in the turbulence model. As depicted by the Figure, and with respect to the results shown in Figure 4, the overestimation of the W/Ts' performance has been partially corrected and the small increase in the performance of the third, fourth and fifth W/Ts when compared to the power performance of the second WT, which is observed in the experimental data, is reproduced by the calculation.

4.2 Wind farm in complex terrain

The second wind farm examined is located in complex terrain in Spain and comprises 43 machines sited in five rows at 11 D distances. The distance between two machines in the same row is 1.5 D. 10 out of the 43 machines feature a higher hub height than the others.

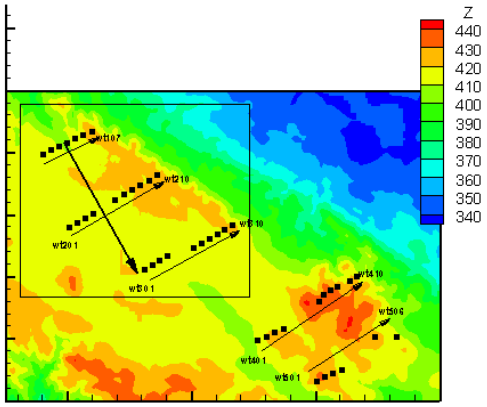

Figure 6: Layout of the complex terrain wind farm. The contours indicate the terrain elevation. The arrow perpendicular to the W/T rows shows the wind direction of 325°.

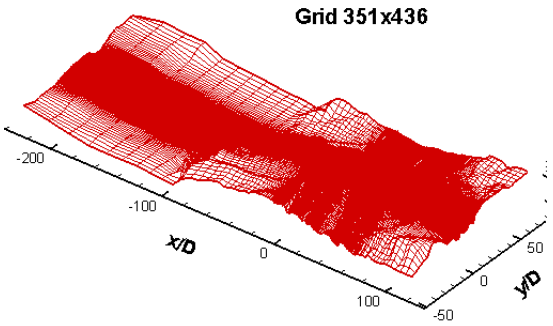

Figure 7: Layout of the surface grid for the wind direction 325° case.

The terrain contours and a layout of the surface grid for the examined case, that corresponds to a wind direction value of 325°, consisting of 351x436 points, are presented in Figure 6 and Figure 7. The 325° direction corresponds to flow nearly perpendicular to the W/T rows. Taking into account that 45 grid lines have been used in the vertical direction, the computational grid consists of nearly 7 million grid points.

As depicted by Figure 7, the inflow boundary of the computational domain has been placed far enough from the locations of the W/Ts, so that the largest possible part of terrain influencing the development of the flow is taken into account. The grid spacing in the x-y plane starts from a minimum value of 0.1 D at the locations of W/Ts and increases outwards using a geometrical progression. In the vertical direction, the first grid line has been positioned at 0.5 m above ground. The grid density over the rotor disk surfaces was properly chosen by performing three runs for the first 3 W/T's rows in a hypothetical flat terrain, with 71, 100 and 134 grid points over each rotor disk surface respectively. A number of 100 grid points was found to be sufficient for grid independent predictions.

To account for the complexity of the terrain a computation is first performed without the WTs (including only the terrain topography), that is used to estimate the yaw angle at each rotor disk. The predicted wind direction at the hub height gives each W/T's orientation. The discretization of each rotor disk is done using the grid cells that fulfil certain geometrical criteria regarding the W/T orientation and the distance from the ground.

The Durbin's correction has been included in the calculation; however, it was found that it does not influence the predictions significantly because of the large distance between the W/Ts.

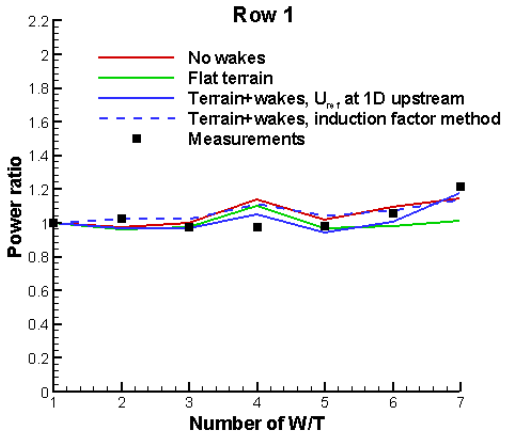

Figure 8: Power ratios of the WTs in the first row, with reference to the first W/T of the first row, for the complex terrain wind farm for wind direction 325°.

The relative power performances of all the wind turbines are compared to the experimental data for the wind direction value of 325° in Figure 8 – Figure 11. All the power ratios refer to the first W/T in the first row.

The measurements have been collected to correspond to a free stream wind speed of 8 m/s for the first W/T in the first row and correspond to natural conditions. Dealing with data from an operational wind farm the dominant sources of uncertainty are mainly caused by lack of calibration for the power converter and yaw position signals. So, the estimation of the reference WT's yaw position was not better than ±5°. The actual power productions are averaged from data covering the range 322° – 332° of wind direction for the the first W/T in the first row.

In all figures, the "no wakes" distributions refer to the predictions without W/Ts that include only the effect of the topography, whilst the "flat terrain" distributions refer to the predictions of the same W/T configuration in flat terrain. In this way, the topography and the wake induced effects are distinguished and can be independently assessed and compared to the power predictions for the complete simulations (that are denoted as "terrain+wakes" in the figures). The "flat terrain" calculations have been performed using the average wind speed at a rotor plane one diameter upstream of the W/T as reference value in the thrust calculation. The complete wind farm calculation has been performed using both methods for the estimation of the reference wind speed.

As depicted by the figures, and in contrast to the flat terrain case, the commonly used method for the estimation of the reference wind

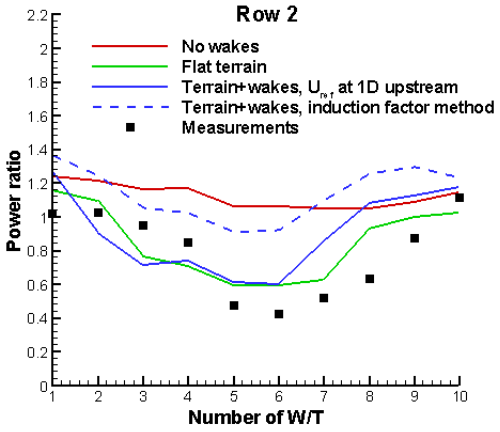

Figure 9: Power ratios of the WTs in the second row, with reference to the first W/T of the first row, for the complex terrain wind farm for wind direction 325°.

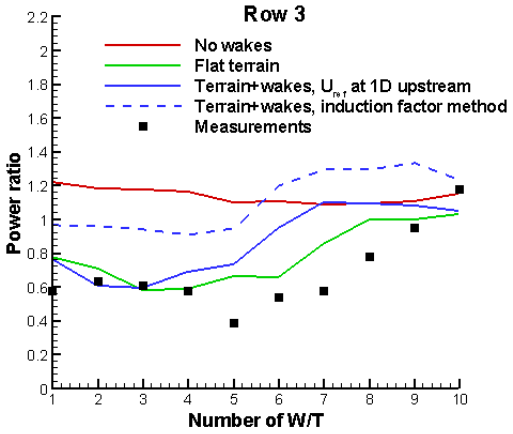

Figure 10: Power ratios of the WTs in the third row, with reference to the first W/T of the first row, for the complex terrain wind farm for wind direction 325°.

speed (one diameter upstream) produces better results than the induction factor-based method, which significantly over-predicts the power ratios of the W/Ts, indicating that its use in complex terrain should be further investigated. Nevertheless, in the distributions by both methods there are significant discrepancies to the measured data, especially for the third row.

One possible reason could be the non-accurate representation of the terrain in the provided digital terrain model (for example, the measured power for the first four machines in the first row are almost identical despite the elevation differences and the fact that the fourth machine features a 10 m higher hub height) or the restrictions set by the present computational capabilities to the use of a finer mesh. Another reason could be

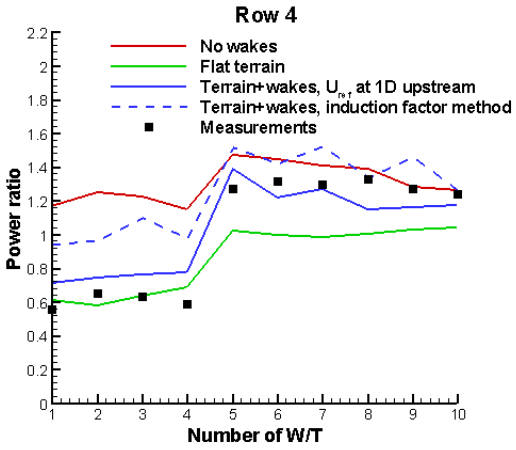

Figure 11: Power ratios of the WTs in the fourth row, with reference to the first W/T of the first row, for the complex terrain wind farm for wind direction 325°.

the non-accurate definition of the reference wind speed for the thrust estimation and the uncertainty of the measured data.

The power reduction for most of the wind turbines at the second and third row comes from the interaction with the upstream W/Ts due to the wake effects; however, the presence of the terrain reduces the wake effect of the preceding W/Ts. At the fourth row, the second group of six W/Ts is not significantly affected by wakes of the preceding turbines, because they are located almost outside of the area that the wakes develop. In addition, they are located at higher terrain altitudes where the topography effect is dominant.

5 Conclusions

CFD modelling of entire wind farms has been presented in this paper. Two wind farms, one in flat and one in complex terrain have been simulated in terms of their performance and wake losses and calculations have been compared against existing measurements. The exercise provided the grounds for investigating two critical modelling issues in W/T wake modelling using CFD: (a) the identified need for turbulence model correction in order to properly model the near-wake velocity deficit and (b) the way that the reference wind speed derives for calculating the thrust of the shadowed WTs and/or WTs located in complex terrain.

In contrast to other corrections proposed as a remedy for (a), the turbulence correction adopted in this work has the advantage of not including any additional parameters requiring

calibration. This is due to the fact that the application of Durbin's model is a rather "natural" correction of the turbulence structure of the braking flow behind the rotor disc when modelled, as in our case, as a perforated disc. In any case, the usual assumption in CFD wake modelling that the rotor is just acting as a momentum sink without any further influence on the Reynolds stress tensor seems inadequate.

Regarding (b), two different approaches have been tested. In the first, the reference wind speed is approximated by means of the wind speed at hub height on a plane situated one diameter upwind from the modelled turbine. The second is based on the induction factor concept. This gives the advantage of avoiding the link of the reference wind speed with a specific upstream distance from the W/T, which is quite arbitrary especially in complex terrain and/or multi-wake simulations.

The combination of the induction factor method and the turbulent model correction produced satisfactory results for the flat terrain case and improved significantly the ability of the present method to reproduce the actual physical patterns. The induction factor method is consistent with the wake deficit under-prediction observed in previous single wake calculations, whilst the Durbin's correction of the turbulence model trimmed the underestimation of the deficit and reproduced the measured decay.

On the contrary, the induction factor method did not produce satisfactory results in the complex terrain case. The measured power ratios were overestimated and the typical method of defining the reference velocity at one diameter upstream produced much better results. It is probable that the induction factor method cannot perform satisfactorily in complex terrain due to its inherent flow uniformity assumptions. The case has to be revisited in all its details including topographical data to assure that the deviations are due to wake modelling and not to the complex terrain flow itself.

References

[1] Lissaman, P.B.S., "Wind Turbine airfoils and rotor wakes," in D. A. Spera (ed.), *Wind Turbine Technology*, ASME Press, New York, 1994, pp. 283-323

[2] Voutsinas, S.G., Rados, K.G. and Zervos, A., "On the Analysis of Wake Effects in Wind Parks," *Wind Engineering*, 1990, 14, pp. 204-219

[3] Abramovich, G.N., *The Theory of Turbulent Jets*, MIT Press, Cambridge, MA, 1963

[4] Taylor, P. A., "On Wake Decay and Row Spacing for WECS Farms," *Proceedings of 3rd International Symposium on Wind Energy Systems*, Lyngby, 1980, pp. 451-468

[5] Crespo, A., Manuel, F., Moreno, D., Fraga, E. and Hernández, J., "Numerical Analysis of Wind Turbine Wakes," *Proceedings of Delphi Workshop on Wind Energy Applications*, Delphi, 1985, pp. 15-25

[6] Tindal, A., Dynamic Loads in Wind Farms, Final Technical Report*, CEC Project JOUR-0084-C*, 1993

[7] Voutsinas, S. G., Rados, K. G. and Zervos A., "Wake Effects of the Rotor Geometry on the Formation and the Development of its Wake," *J. Wind Eng. Ind. Aerodyn.*, 1992, 39, pp. 293-301

[8] Larsen, G. C., Madsen, H.A., Tompsen, K., Larsen, T.J., "Wake Meandering: A Pragmatic Approach", *Wind Energy*, 2008, 11, pp. 377-395

[9] Sørensen, J. N., and Shen, W. Z., "Numerical Modelling of Wind Turbines," *J. Fluids Engineering*, 2002, 124, pp. 393-399

[10] Barthelmie, R.J., Hansen, K, Frandsen, S.T., Rathmann, O., Schepers, J.G., Schlez, W., Phillips, J., Rados, K., Zervos, A., Politis, E.S., and Chaviaropoulos, P.K., "Modelling and Measuring Flow and Wind Turbine Wakes in Large Wind Farms Offshore", *Wind Energy*, Vol. 12, No. 5, pp. 431-444, 2009

[11] Troen, I., Petersen, E.L., *European Wind Atlas*, Risø National Laboratory, Roskilde, Denmark, 1989:656

[12] Schepers, J.G., *ENDOW: Validation and Improvement of ECN's Wake Model*. ECN:ECN-C-03-034: Petten, The Netherlands, 2003: 113

[13] Crespo, A., Hernandez, J., Fraga, E., Andreu, C., "Experimental validation of the UPM computer code to calculate wind turbine wakes and comparison with other models", *Journal of Wind Engineering and Industrial Aerodynamics*, 1988, 27, pp. 77-88

[14] Rados, K., Larsen, G., Barthelmie, R., Schelz, W., Lange, B., Schepers, G., Hegberg, T., Magnusson, M., "Comparison of wake

models with data for offshore windfarms", *Wind Engineering*, 2002, 25, pp. 271-280

[15] Chaviaropoulos, P. K. and Douvikas, D. I., "Mean-flow-field Simulations over Complex Terrain Using a 3D Reynolds Averaged Navier–Stokes Solver," *Proceedings of ECCOMAS '98*, 1998, Vol. I, Part II, pp. 842-848

[16] Prospathopoulos, J.M., Politis, E.S., Chaviaropoulos, P.K., "Modelling wind turbines in complex terrain", Proceedings of the 2008 European Wind Energy Conference & Exhibition, Brussels, 31/3-3/4/2008, Edited by P. K. Chaviaropoulos, pp. 42-46.

[17] Stull, R. B., "An introduction to boundary layer meteorology", ISBN 90-277-2768-6 ed. Kluwer Publications Ltd, 1988

[18] Panofsky, H., Dutton, J., "Atmospheric Turbulence" Wiley, New York, 1984

[19] El Kasmi, A., and Masson, C., "An extended k-ε model for turbulent flow through horizontal axis wind turbines", J. of Wind Eng. Ind. Aerodyn., 2008, 96, pp.103-122.

[20] Politis, E.S., Rados, K., Prospathopoulos, J., Chaviaropoulos, P.K., Zervos, A., "CFD modeling issues of wind turbine wakes under stable atmospheric conditions", poster at EWEC 2009, Marseille, France, March 16-19, 2009.

[21] Durbin, P.A., "On the k-ε stagnation point anomaly", *Int. J. Heat and Fluid Flow*, 1996, 17(1), pp.89-90

[22] Eggleston, D.M., and Stoddard, F.S., Wind Turbine Engineering Design, Van Nostrand Reinhold, New York, pp. 30–35, 58, 1987

[23] Machielse, L.A.H., Eecen, P.J., Korterink, H., van der Pijl, S.P. and Schepers, J.G., "ECN Test Farm Measurements For Validation of Wake Models", Proceedings of the 2007 European Wind Energy Conference & Exhibition, Milan 7-10/5/2007, Edited by P. K. Chaviaropoulos, pp. 98-102